

# Discovery of metastable states in a finite-size classical one-dimensional planar spin chain with competing nearest- and next-nearest-neighbor exchange couplings

Alexander P. Popov,<sup>1</sup> Angelo Rettori,<sup>2,3</sup> and Maria Gloria Pini<sup>4,\*</sup><sup>1</sup>*Department of Molecular Physics, National Research Nuclear University MEPhI, 115409 Moscow, Russia*<sup>2</sup>*Dipartimento di Fisica ed Astronomia, Università di Firenze, I-50019 Sesto Fiorentino (FI), Italy*<sup>3</sup>*Centro S3, c/o Istituto Nanoscienze del CNR (CNR-NANO), I-41125 Modena, Italy*<sup>4</sup>*Istituto dei Sistemi Complessi del CNR (CNR-ISC), Unità di Firenze, I-50019 Sesto Fiorentino (FI), Italy*

(Received 5 August 2014; revised manuscript received 2 October 2014; published 22 October 2014)

A theoretical method recently developed is used to find all possible equilibrium magnetic states of a finite-size classical one-dimensional planar spin chain with competing nearest-neighbor (nn) and next-nearest-neighbor (nnn) exchange interactions. The energy of a classical planar model with  $N$  spins is a function of  $N$  absolute orientational angles or equivalently, due to the absence of in-plane anisotropy, of  $(N - 1)$  relative orientational angles. The lowest energy stable state (ground state) corresponds to a global minimum of the energy in the  $(N - 1)$ -dimensional space, while metastable states correspond to local minima. For a given value of the ratio,  $\gamma$ , between nnn and nn exchange couplings, all the equilibrium configurations of the model were calculated with great accuracy for  $N \leq 16$ , and a stability analysis was subsequently performed. For any value of  $N$ , the ground state was found to be “symmetric” with respect to the middle of the chain in the relative angles representation. For the chosen value of  $\gamma$ , the ground state consists of a helix whose chirality is constant in sign along the chain (i.e., all the spins turn clockwise, or all anticlockwise), but whose pitch varies owing to finite-size effects; e.g., for positive chirality we found that the chiral order parameter  $\chi(N) > 0$  increases monotonically with increasing  $N$ , approaching the value ( $\chi = 1$ ) pertinent to the ground state in the limit  $N \rightarrow \infty$ . For finite but not too small values of  $N$ , we found metastable states characterized by one reversal of chirality, either localized just in the middle of the chain [“antisymmetric” state, with chiral order parameter  $\chi(N) = 0$ ], or shifted away from the middle of the chain, to the right or to the left [pairs of “ugly” states, with equal and opposite values of  $\chi(N) \neq 0$ ; the attribute “ugly” refers to the absence of a definite symmetry in the relative angles representation]. Concerning the stability of these states with one reversal of chirality, two main results were found. First, the “antisymmetric” state is metastable for even  $N$  and unstable for odd  $N$ . Second, an additional pair of “ugly” states is found whenever the number of spins in the chain is increased by 1; the states in each additional pair are unstable for even  $N$  and metastable for odd  $N$ . Analysis of stable and metastable configurations in the framework of a discrete nonlinear mapping approach provides further support for the above results.

DOI: [10.1103/PhysRevB.90.134418](https://doi.org/10.1103/PhysRevB.90.134418)

PACS number(s): 75.10.Hk, 75.10.Pq, 75.60.Ch

## I. INTRODUCTION

Phase transitions are accompanied by spontaneous symmetry breaking. The situation may be very complex in frustrated systems, where both continuous and discrete symmetries are present at the same time. In some rare-earth magnetic systems, such as Ho, Dy, and Tb [1], as well as in many alloys, such as MnAu<sub>2</sub> [2,3], frustration is due to the fact that along a certain direction the nearest-neighbor (nn) exchange interaction ( $J_1$ ) competes with the next-nearest-neighbor (nnn) one ( $J_2$ ):

$$\mathcal{H} = \sum_i (-J_1 \mathbf{S}_i \cdot \mathbf{S}_{i+1} - J_2 \mathbf{S}_i \cdot \mathbf{S}_{i+2}). \quad (1)$$

Assuming, e.g.,  $J_1 > 0$  and  $J_2 < 0$ , the ground state in the thermodynamic limit turns out [4–6] to be ferromagnetic if  $\gamma = J_2/J_1 \geq -1/4$ . In contrast, for  $\gamma < -1/4$  the ground state is a modulated helical phase, with a critical wave vector  $\mathbf{Q}$  whose modulus determines the constant angle  $\bar{\alpha}$  between two neighboring spins ( $a$  is the lattice constant):

$$\cos(Qa) = -\frac{1}{4\gamma} = \frac{J_1}{4|J_2|} = \cos \bar{\alpha}. \quad (2)$$

Clearly, a right-hand and a left-hand helix with pitch  $\pm\bar{\alpha}$  are energetically degenerate. Following Villain [7], the helical ground state is characterized, in addition to the local spin variable  $\mathbf{S}_i$ , by another order parameter: the vector chirality  $\boldsymbol{\kappa}_i$ , which is related to the mutual orientation of spins on neighboring sites,

$$\boldsymbol{\kappa}_i = \frac{\mathbf{S}_i \times \mathbf{S}_{i+1}}{\sin \bar{\alpha}}. \quad (3)$$

In the case, considered in the present work, of a planar spin chain, the spins are confined to lie in a plane ( $xy$ ) perpendicular to the chain direction ( $z$ ), so the chirality has just the  $z$  component which, for  $T = 0$ , takes only the values  $\kappa_i^z = \pm 1$  (like an Ising variable) on each lattice site. For a planar spin chain of  $N$  spins one can define the chiral order parameter,  $\chi(N)$ , in terms of the sum

$$\chi(N) = \frac{1}{N-1} \sum_{i=1}^{N-1} \kappa_i^z. \quad (4)$$

In the thermodynamic limit  $N \rightarrow \infty$ , the helical ground state has a twofold chiral degeneracy, in addition to the usual continuous spin rotation degeneracy: the onset of helical order is related to spontaneous breaking of the  $Z_2 \times \text{SO}(2)$  symmetry [8]. In some cases, it is even possible that the helical

\*mariagloria.pini@isc.cnr.it

ground state is reached via a two-step magnetic ordering mechanism [9]. For systems described by Hamiltonian (1), many studies were addressed [1,10–12] to find the stable configurations at  $T = 0$ . In the limit  $N \rightarrow \infty$ , in addition to the doubly degenerate helical ground state with constant helix pitch  $\bar{\alpha}$  given by Eq. (2), two kinds of nonuniform magnetic configurations were found [11,12] by transforming (1) into a continuum functional and solving it by analytical methods, namely, (i) isolated domain walls between helical spin arrangements with the same pitch and opposite chirality, and (ii) modulated structures with periodically alternating chirality. It is interesting to note that the latter structures are similar to the multisoliton solutions investigated by Aubry [13] in the discrete Frenkel-Kontorova (FK) model [14] which, as model (1), includes incommensurability and frustration in a natural way. It was proved some years ago [15] that the FK model falls out of equilibrium when cooled at a finite rate. Thus, it may happen that the system freezes into some metastable configurations, corresponding to local minima of the energy. It is curious to observe that a similar phenomenon of metastability can occur in quite different nonmagnetic systems, such as stretched elastomer strips. In fact, helical structures characterized by a single reversal or multiple reversals of chirality were experimentally found to be metastable [16] depending on the strip's cross section. In that context, the reversals of chirality were named “perversions” [17], and the metastable helical structures “hemihelices” [16].

In recent times, the availability of very sophisticated growth and characterization techniques allowed the study of the behavior of ultrathin magnetic films, and thus the investigation of the consequences of the loss of translational invariance in the direction normal to the film plane. Nanometric objects are very important not only on the fundamental point of view, but also for their implementation in nanotechnologies. Even in the case of rare-earth elements, such as Ho and Dy, ultrathin films could be obtained [18,19] whose thickness is comparable with the modulation period of the helix. Moreover, striking effects such as the onset of a block phase [20], where outer ordered layers coexist with inner disordered ones, are expected as the temperature is varied. Also thin films of antiferroelectric liquid crystals [21] can be modeled by Hamiltonian (1). In Fe/Ni bilayers grown epitaxially on Cu(100), Néel-type domain walls with fixed chirality were recently observed [22] in the magnetic stripe phase, depending on the film growth order (right-handed in Fe/Ni bilayers and left-handed in Ni/Fe bilayers). Another recent experimental investigation, performed using spin-polarized scanning tunneling microscopy in Fe chains deposited on the  $(5 \times 1)$  reconstructed surface of Ir, displayed a spiral magnetic order; it was suggested that the latter could provide a new transport mechanism based on chirality [23].

Within this context, we aim at investigating all possible stable states of model (1) in the presence of a finite number of spins,  $N$ . In particular, for a given value of the ratio  $\gamma = J_2/J_1$ , we will consider the case  $N \approx \frac{2\pi}{\bar{\alpha}}$ ; i.e., the size of the chain is comparable with the period of helix modulation of an infinite chain with the same value of  $\gamma$ . We will assume a 1D planar model, with the spins confined to a plane ( $xy$ ) perpendicular to the chain axis ( $z$ ). In the presence of competing nearest-neighbor ( $J_1 > 0$ ) and next-nearest-

neighbor ( $J_2 < 0$ ) exchange interactions, the energy then reads

$$E(N) = -J_1 \sum_{i=1}^{N-1} \cos(\theta_i - \theta_{i+1}) - J_2 \sum_{i=1}^{N-1} \cos(\theta_i - \theta_{i+2})(1 - \delta_{i,N-1}), \quad (5)$$

where  $\theta_i$  ( $i = 1, \dots, N$ ) denotes the absolute angle formed by the spin  $\mathbf{S}_i$  with the  $x$  axis. The spins are supposed to be classical vectors of unit length:  $S_i^x = \cos \theta_i$ ,  $S_i^y = \sin \theta_i$ . Equivalently, in terms of the relative angles  $\alpha_i = \theta_{i+1} - \theta_i$  ( $i = 1, \dots, N-1$ ), one can rewrite Eq. (5) in the reduced (and more symmetric) form

$$\epsilon(N) = \frac{E(N)}{J_1} = - \sum_{i=1}^{N-1} \cos \alpha_i - \frac{\gamma}{2} \sum_{i=1}^{N-1} \cos(\alpha_{i-1} + \alpha_i)(1 - \delta_{i,1}) - \frac{\gamma}{2} \sum_{i=1}^{N-1} \cos(\alpha_i + \alpha_{i+1})(1 - \delta_{i,N-1}). \quad (6)$$

In this paper, we will consider the case  $\gamma = J_2/J_1 \lesssim -1/4$ . The chiral order parameter,  $\chi(N)$ , of a finite chain with  $N$  spins can be explicitly expressed in terms of the  $N-1$  relative angles,  $\alpha_i$ , as

$$\chi(N) = \frac{\sum_{i=1}^{N-1} \sin \alpha_i}{(N-1) \sin \bar{\alpha}}. \quad (7)$$

Notice that in (5), or equivalently in (6), open boundary conditions were introduced through the Kronecker's delta functions.

Regarding the applicability of model (5) to real magnetic systems, such as ultrathin magnetic films or chains of magnetic adatoms on metal surfaces, we observe that the presence of a magnetic anisotropy and possibly an external magnetic field should in principle be taken into account, leading one to consider energy terms dependent on the spin orientation of single atoms, in addition to the interactions between nn and nnn spin pairs. The study of such an extended model is deferred to future work since, as shown by Belobrov *et al.* [24] in the case of an infinite chain, it requires some attention particularly with regard to magnetic anisotropy. As for an additional external field, a very weak one is not expected to change the stable states in a relevant way. In fact, considering that the finite spin chain turns out to have a nonzero magnetization, a weak field will essentially rotate the whole magnetic structure as a giant molecule, tending to align its vector magnetization along the field direction. This rotation takes place due to the interactions of the spin chain with a thermal bath, in accordance with the relaxation mechanism involved in the reorientation process.

Other phenomenological models which allow one to describe a magnetic helical state, e.g., a model where the antisymmetric Dzialoshinskii-Moriya interaction [25,26] (DMI)

$$E_{\text{DM}} = \sum_{i,j} \mathbf{D}_{ij} \cdot (\mathbf{S}_i \times \mathbf{S}_j) \quad (8)$$

competes with symmetric exchange, will be considered in a future publication. Actually, low-dimensional systems lack structural inversion symmetry owing to the presence of interfaces and surfaces, and the effect of including DMI is expected to be that of breaking the chiral symmetry, giving rise to a homochiral spin structure. However, such a structure has generally a long period with respect to the lattice constant [27].

It appears that, in the regime of finite size for model (6), it is mandatory to take into account the discreteness of the chain. In this work this task is accomplished using a theoretical method [28,29] which was recently developed to find, in a very accurate way, the noncollinear canted magnetic states of ultrathin films with competing surface and bulk anisotropies. The method is presented in Sec. II. It is based on the fact that imposing the necessary conditions for minima of the energy to exist, the so-obtained set of equations for orientational angles allow one to express all the angles in terms of just the first one. After the substitution of these angles in the expression for the energy, the latter becomes a function of only one parameter, the first orientational angle. Plotting the energy versus the first orientational angle allows one to visualize both local and global minima of the energy. Standard subsequent analysis of these minima leads one to establish which are the stable, metastable, and unstable magnetic states of the chain.

The main results obtained in the present work are presented in Sec. III and can be summarized as follows. For a given value of the ratio,  $\gamma$ , between nnn and nn exchange couplings, all the equilibrium configurations of the model were calculated with great accuracy for  $N \leq 16$ , and a stability analysis was subsequently performed. For any value of  $N$ , the ground state was found to be “symmetric” with respect to the middle of the chain in the relative angles representation. For the chosen value of  $\gamma$ , the ground state consists of a helix whose chirality does not change, but whose pitch varies owing to finite-size effects. For finite but not too small values of  $N$ , we found metastable states characterized by one reversal of chirality. The reversal can be either localized just in the middle of the chain [“antisymmetric” state, with chiral order parameter  $\chi(N) = 0$ ], or shifted away from the middle of the chain, to the right or to the left [pairs of “ugly” states, with equal and opposite values of  $\chi(N) \neq 0$ ]. The attribute “ugly” was chosen referring to the absence of a definite symmetry in the relative angles representation. Concerning the stability of these states with one reversal of chirality, two main results were found. First, the “antisymmetric” state is metastable for even  $N$  and unstable for odd  $N$ . Second, an additional pair of “ugly” states is found whenever the number of spins in the chain is increased by 1; the states in each additional pair are unstable for even  $N$  and metastable for odd  $N$ . A discrete nonlinear mapping approach provides further support for the above results. Clearly such even-odd effects, being a consequence of discretization, cannot be evidenced using a continuous approximation to Eq. (5) or (6). However, they may be important when the model is applied to the investigation of real systems.

In Sec. IV we present another theoretical formulation of the problem, based on a nonlinear mapping approach [24,30–32] in the appropriate phase space, where the discreteness of the lattice is preserved. This method is useful since it is based on very general principles, originally developed in the study of dynamical systems, and it provides an overview of all

equilibrium states of the system in terms of a phase portrait. Belobrov *et al.* [24] performed such an analysis for classical models of spin chains in the limit  $N \rightarrow \infty$ , while Trallori *et al.* [30] showed that the equilibrium configurations of a finite open chain can be represented by trajectories of a nonlinear mapping satisfying opportune boundary conditions. In the case of our model (6), the various roots (obtained in Sec. III using the method described in Sec. II) are then revisited in Sec. IV in terms of the topological properties of such trajectories. Finally, the conclusions are drawn in Sec. V.

## II. THEORETICAL METHOD TO FIND THE $T = 0$ MAGNETIC STRUCTURE

Starting from Eq. (6), the equilibrium configurations for the open chain with  $N$  spins are obtained imposing the following  $(N - 1)$  conditions on the  $(N - 1)$  relative angles  $\alpha_i$ :

$$\begin{aligned} \frac{\partial \epsilon}{\partial \alpha_i} = 0 = & \sin \alpha_i + \gamma \sin(\alpha_{i-1} + \alpha_i)(1 - \delta_{i,1}) \\ & + \gamma \sin(\alpha_i + \alpha_{i+1})(1 - \delta_{i,N-1}) \quad (1 \leq i \leq N - 1). \end{aligned} \quad (9)$$

The essence of the method [28] is to use the  $i$ th equation to express  $\alpha_{i+1}$  in terms of  $\alpha_i$  and  $\alpha_{i-1}$ , for  $i = 1, \dots, (N - 2)$ . For the chain of  $N$  spins in Eq. (5), involving  $(N - 1)$  relative angles in Eq. (6), one has explicitly

$$\begin{aligned} \alpha_2 = & -\alpha_1 + \arcsin \left[ -\frac{1}{\gamma} \sin \alpha_1 \right] \quad \text{for } i = 1, \\ \alpha_{i+1} = & -\alpha_i + \arcsin \left[ -\frac{1}{\gamma} \sin \alpha_i - \sin(\alpha_{i-1} + \alpha_i) \right] \\ & \quad \text{for } 2 \leq i \leq N - 3, \\ \alpha_{N-1} = & -\alpha_{N-2} + \arcsin \left[ -\frac{1}{\gamma} \sin(\alpha_{N-2}) \right. \\ & \left. - \sin(\alpha_{N-3} + \alpha_{N-2}) \right] \quad \text{for } i = N - 2. \end{aligned} \quad (10)$$

It is important to note that in writing the previous  $(N - 2)$  equations, we have always taken the principal value of the  $\arcsin(y)$  function, defined as the solution of equation  $\sin(x) = y$  in the interval  $x \in [-\pi/2, +\pi/2]$ . This is justified provided that the nnn antiferromagnetic interaction ( $J_2 < 0$ ) does not dominate in the system so that,  $\forall i$ , the condition  $(\alpha_i + \alpha_{i+1}) < \pi/2$  is fulfilled. Otherwise, the other branch  $x = \pi - \arcsin(y)$  has to be taken. Moreover, we observe that if the system of Eqs. (9) is satisfied by the set of positive angles  $\alpha_i > 0$  ( $i = 1, \dots, N - 1$ ), then it is satisfied by the set of negative angles ( $-\alpha_i < 0$ ), too. Therefore, in the following we will consider only positive angles.

Now we draw the reader’s attention to the fact that, to obtain the  $(N - 2)$  equations in the set (10), we did *not* use the last  $(N - 1)$ th equation in the set (9). Therefore, the set (10) determines a line in the  $(N - 1)$ -dimensional space of angles  $\alpha_1, \alpha_2(\alpha_1), \dots, \alpha_{N-1}(\alpha_1)$ . When these  $(N - 1)$  angles are substituted in the expression for the reduced energy (6), the latter takes the form of a function of only the first angle,  $\alpha_1$ :

$$\Phi(\alpha_1) \equiv \epsilon[\alpha_1, \alpha_2(\alpha_1), \dots, \alpha_{N-1}(\alpha_1)]. \quad (11)$$

In this way, the rather complex problem of finding the minima of energy in the  $(N - 1)$ -dimensional space of angles  $\alpha_1, \alpha_2, \dots, \alpha_{N-1}$  is reduced to the much simpler problem of finding the minima of a function,  $\Phi(\alpha_1)$ , of only one argument, the first angle  $\alpha_1$ . This function can be plotted and its minima are easily visualized.

However, it must be realized that the minima of  $\Phi(\alpha_1)$  are not necessarily also minima of the reduced energy (6), because the last of Eqs. (9) was not used to construct the function  $\Phi(\alpha_1)$ . The first derivative of  $\Phi(\alpha_1)$  is

$$\begin{aligned} \frac{d\Phi(\alpha_1)}{d\alpha_1} = & \frac{\partial\epsilon}{\partial\alpha_1} + \frac{\partial\epsilon}{\partial\alpha_2} \frac{\partial\alpha_2}{\partial\alpha_1} + \dots \\ & + \frac{\partial\epsilon}{\partial\alpha_{N-2}} \frac{\partial\alpha_{N-2}}{\partial\alpha_1} + \frac{\partial\epsilon}{\partial\alpha_{N-1}} \frac{\partial\alpha_{N-1}}{\partial\alpha_1}, \end{aligned} \quad (12)$$

where, by construction, all the terms in the summation on the right-hand side are zero, except the last one. Now we observe that the condition  $d\Phi(\alpha_1)/d\alpha_1 = 0$  can be satisfied in either of the two cases: (i)  $\partial\epsilon/\partial\alpha_{N-1} = 0$ ; or (ii)  $\partial\epsilon/\partial\alpha_{N-1} \neq 0$ , but  $\partial\alpha_{N-1}/\partial\alpha_1 = 0$ . Let us now define the function  $F(\alpha_1)$  of only the first angle  $\alpha_1$  as follows:

$$\begin{aligned} F(\alpha_1) \equiv & \frac{\partial\epsilon}{\partial\alpha_{N-1}} = \sin[\alpha_{N-1}(\alpha_1)] \\ & + \gamma \sin[\alpha_{N-2}(\alpha_1) + \alpha_{N-1}(\alpha_1)]. \end{aligned} \quad (13)$$

Clearly, among the minima of  $\Phi(\alpha_1)$ , only those satisfying  $F(\alpha_1) = 0$  [i.e., satisfying the last equation in the set (9)] can be minima also of the energy (6). Therefore, to find the minima of the energy of a classical planar chain of  $N$  spins with competing nn and nnn exchange constants, we adopt the following operative procedure:

(1) We numerically solve the equation  $F(\alpha_1) = 0$  with the desired degree of accuracy and we obtain the first relative angle  $\alpha_1^{(0)}$ . Clearly, for a given interval of  $\alpha_1$ , one will find several zeros of the function  $F(\alpha_1)$ . Then, using the set of  $(N - 2)$  Eqs. (10), from  $\alpha_1^{(0)}$  we determine the remaining relative angles  $\alpha_i^{(0)}$ , with  $i = 2, \dots, N - 1$ .

(2) We substitute the so-obtained configuration in Eq. (11). We plot the function  $\Phi(\alpha_1)$  versus  $\alpha_1$  and determine its global and local minima.

(3) We perform a stability analysis to determine whether a given stationary configuration,  $\alpha_i^{(0)}$  ( $i = 1, \dots, N - 1$ ), corresponds to a stable, metastable, or unstable state of the finite chain. Namely, for each configuration of relative angles, we calculate the eigenvalues of the matrix  $A_{mn} \equiv \partial^2\epsilon/(\partial\alpha_m\partial\alpha_n)|^{(0)}$ . If all eigenvalues are negative, the configuration corresponds to a maximum of the energy. If, among the  $N - 1$  eigenvalues of the Hessian matrix  $A_{mn}$ , at least one negative eigenvalue is found, the configuration is rejected as unstable (saddle point of the energy surface). If all eigenvalues are positive, the configuration corresponds to a minimum of the energy, either global (the ground state) or local (a metastable state).

(4) For each configuration of relative angles  $\alpha_i^{(0)}$  ( $i = 1, \dots, N - 1$ ) corresponding to a global or local minimum of the energy, we obtain the corresponding configuration of absolute angles  $\theta_i^{(0)}$  ( $i = 1, \dots, N$ ).

### III. RESULTS

Using the theoretical method described in the previous section, we have calculated the minima of the energy for the model (5), or equivalently (6), of an open chain with a finite number,  $N$ , of spins in the case  $\gamma = J_2/J_1 = -0.34$ . In Table I we summarize our results on the existence and stability of magnetic states in chains of various length, in the range  $4 \leq N \leq 16$ . In the Appendix we provide a table with the calculated values of all nonzero solutions of equation  $F(\alpha_1) = 0$  [where the function  $F(\alpha)$  is defined in Eq. (13)] for an open chain with  $N = 16$  spins, together with the energies of the corresponding magnetic structures.

In Fig. 1 we provide a schematic view of the zeros of the function  $F(\alpha_1)$ , namely the solutions of the last equation in the set (9), in three special cases ( $N = 12, 13$ , and  $14$ ). In Fig. 2 and Fig. 3 we show all the (stable, metastable, and unstable) configurations of an open chain with  $N = 12$  and  $N = 13$

TABLE I. Stable/metastable (+) and unstable (−) configurations of an open chain with  $\gamma = J_2/J_1 = -0.34$  and a finite number of spins,  $N$ , ranging from 4 to 16. The absence of  $\pm$  symbols in a cell denotes the absence of the related configuration. The leftmost column denotes the unstable collinear ferromagnetic state ( $FM$ ), while the rightmost column denotes the noncollinear ground state (lowest energy stable state,  $S-1$ ).

$N$	$FM$	$AS-2$	$S-2$	$U_{-1}^A$	$U_{-1}^B$	$U_{-1}^C$	$U_{-1}^D$	$U_{-1}^E$	$AS-1$	$U_{+1}^E$	$U_{+1}^D$	$U_{+1}^C$	$U_{+1}^B$	$U_{+1}^A$	$S-1$
4	−														+
5	−														+
6	−														+
7	−								−						+
8	−								−						+
9	−								−						+
10	−		−						−						+
11	−		−						−						+
12	−		−	−					+					−	+
13	−	−	−	−	+				−				+	−	+
14	−	−	−	−	+	−			+			−	+	−	+
15	−	−	−	−	+	−	+		−		+	−	+	−	+
16	−	−	−	−	+	−	+	−	+	−	+	−	+	−	+

spins, respectively. The configurations are reported both in terms of relative angles  $\alpha_i$  ( $i = 1, \dots, N - 1$ ), on the left column, and of absolute angles  $\theta_i$  ( $i = 1, \dots, N$ ), on the right column. We remind the reader that, from each configuration shown in the figures, one can obtain another configuration (not shown) with the same reduced energy,  $\epsilon(N)$ , and opposite chiral order parameter,  $\chi(N)$ , simply by replacing  $\alpha_i$  by its opposite  $-\alpha_i, \forall i = 1, \dots, N - 1$ .

In general, one can distinguish three types of solutions:

(1) ‘‘Symmetric’’ solutions, characterized by  $\alpha_{N-i} = \alpha_i$ , with  $i = 1, \dots, N - 1$ .

(2) ‘‘Antisymmetric’’ solutions, characterized by  $\alpha_{N-i} = -\alpha_i$ , with  $i = 1, \dots, N - 1$ .

(3) ‘‘Ugly’’ solutions, for which the relative angles  $\alpha_i$  ( $i = 1, \dots, N - 1$ ) do not show any particular symmetry with respect to the middle of the chain. However, one should note that ‘‘ugly’’ solutions always come in pairs (connected by a segment in Fig. 1) and that, denoting by (+) and (−) the two solutions belonging to a given pair, one has  $\alpha_{N-i}^{(+)} = -\alpha_i^{(-)}$ .

Before discussing in more detail the various types of configurations of the finite chain, we would like to remark that the ‘‘symmetry’’ or ‘‘antisymmetry’’ of the solutions refers only to their representation in terms of the relative angles  $\alpha_i$ , and not in terms of the absolute angles  $\theta_i$ , as is apparent comparing the left and the right column in Fig. 2 and Fig. 3.

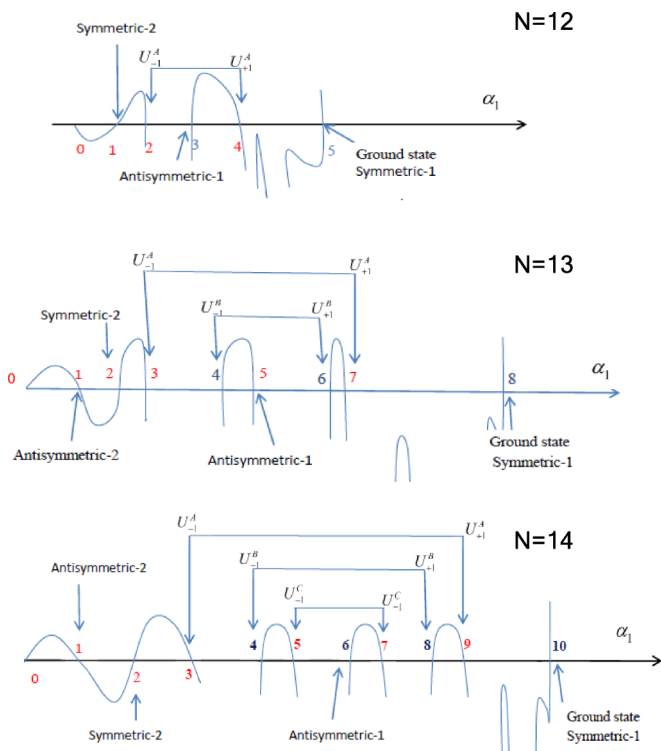


FIG. 1. (Color online) Schematic view of the zeros of the function  $F(\alpha_1)$ , defined in Eq. (13), for an open chain of  $N$  spins with competing nn and nnn exchange coupling. The value of  $\gamma = J_2/J_1 = -0.34$  was kept fixed while  $N$  was varied. The various types of solutions are labeled on the basis of their symmetry with respect to the middle of the chain (‘‘symmetric’’, ‘‘antisymmetric’’, or ‘‘ugly’’) and of their stability/instability (blue/red color of the label). Note that ‘‘ugly’’ solutions always come in pairs ( $U_{\pm}$ ).

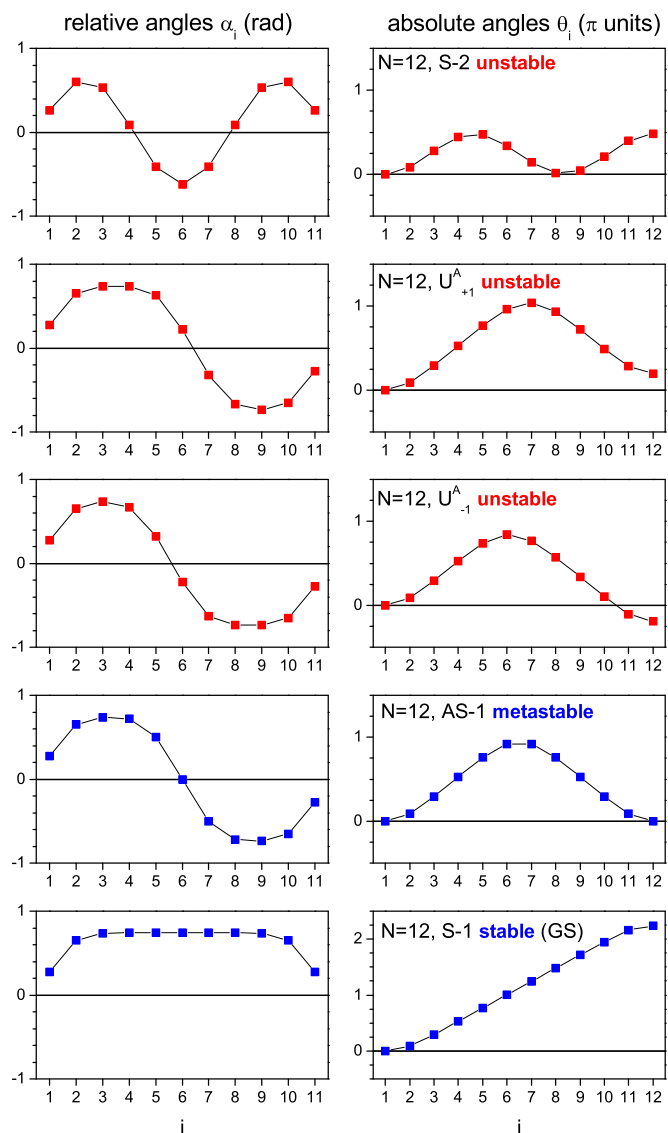


FIG. 2. (Color online) All (stable and metastable, in blue; unstable, in red) configurations for a chain with  $\gamma = -0.34$  and  $N = 12$  spins. Left column: relative angles  $\alpha_i$  ( $i = 1, \dots, N - 1$ ). Right column: absolute angles  $\theta_i$  ( $i = 1, \dots, N$ ). The lines are guides to the eye.

‘‘Symmetric’’ configurations. As regards the ‘‘symmetric’’ configurations, for all values of  $N$  we find that the  $S-1$  state is stable and has the lowest energy; i.e., it is the ground state (GS). For  $10 \leq N \leq 16$  we find another ‘‘symmetric’’ configuration,  $S-2$ , which is higher in energy and unstable. Note that the ground state has a nonuniform profile of the relative angles. In fact, owing to open boundary conditions and finite-size effects,  $\alpha_i$  depends on the position  $i$  along the chain, with increasing deviations of the relative angles from the bulk value  $\bar{\alpha}$ , given in Eq. (2), as  $i$  approaches the end points of the chain. The chiral order parameter in the GS with positive chirality is  $0 < \chi(N) < 1$ , and for increasing  $N$  it is found to increase monotonically, approaching the infinite chain limit ( $\chi = 1$ ) as shown in Fig. 4.

‘‘Antisymmetric’’ configurations. As regards the ‘‘antisymmetric’’ configuration  $AS-1$ , we find that its existence and

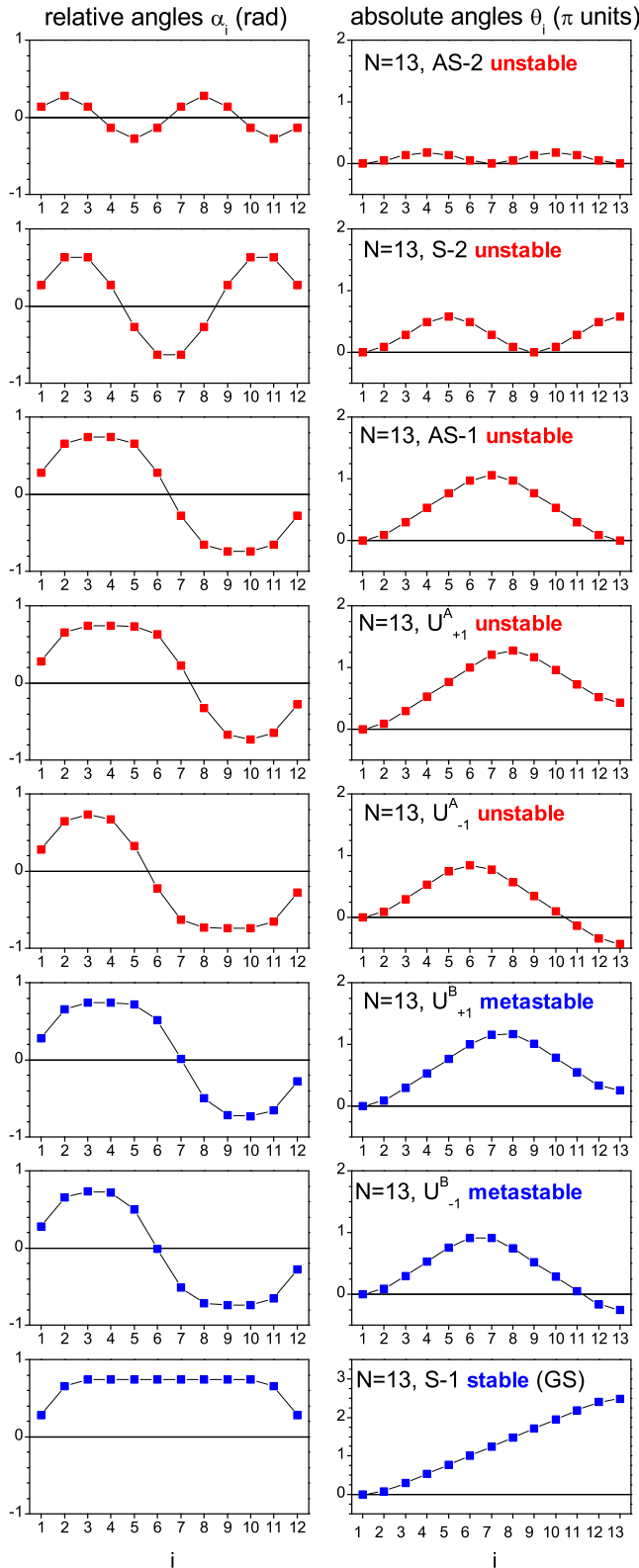


FIG. 3. (Color online) All (stable and metastable, in blue; unstable, in red) configurations for a chain with  $\gamma = -0.34$  and  $N = 13$  spins. Left column: relative angles  $\alpha_i$  ( $i = 1, \dots, N - 1$ ). Right column: absolute angles  $\theta_i$  ( $i = 1, \dots, N$ ). The lines are guides to the eye.

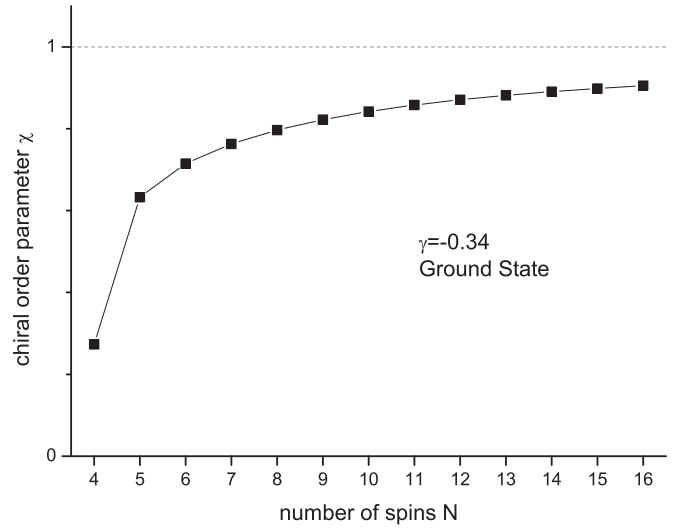


FIG. 4. Chiral order parameter  $\chi$  of the ground-state configuration of a chain with  $\gamma = -0.34$  versus the number,  $N$ , of spins, as calculated from Eq. (7). One has  $\chi(N) > 0$  for a configuration with  $\alpha_i > 0$  ( $i = 1, \dots, N - 1$ ). The line is a guide to the eye.

stability depend on the number of spins,  $N$ , in the chain. More precisely, in the case of a chain with  $\gamma = -0.34$  the AS-1 state is present provided that  $N \geq 7$ , and for small values of  $N$  it is unstable. For higher values of  $N$ , its stability is found to depend on the parity of  $N$ : for even  $N$  the AS-1 state is metastable, while for odd  $N$  it is unstable. These features are illustrated in Fig. 5 and Fig. 6, respectively: the “antisymmetric” AS-1 state exists and is unstable for  $7 \leq N \leq 11$ , while for  $12 \leq N \leq 16$  it is metastable provided that  $N$  is even. Moreover, from Table I and Fig. 3 we observe that for sufficiently long chains ( $N \geq 13$ ) another “antisymmetric” state with higher energy appears, AS-2, which is unstable.

In order to understand the even-odd behavior of the AS-1 state, let us first notice that the chiral order parameter of this “antisymmetric” state is exactly  $\chi = 0$ , owing to the presence of a domain wall located just at the middle of the chain, between regions with opposite chirality. On general grounds, one expects that the AS-1 configuration will be metastable provided that the energy cost of such a chiral domain wall is not too high and surface effects are not too strong. The energy cost of the chiral domain wall depends on the ratio  $\gamma$ ; e.g., when the nnn antiferromagnetic exchange does not dominate over the nn ferromagnetic one, as is the case when  $\gamma = -0.34$ , a configuration where two nearest-neighbor spins in the core of the chiral domain wall are exactly parallel will be energetically favored, and a configuration where two next-nearest-neighbor spins are exactly parallel will be energetically disfavored. For even  $N$ , it is apparent that the condition  $\chi = 0$  implies by symmetry  $\alpha_{\frac{N}{2}} = 0$  (in the relative angles representation), corresponding to an energetically favored configuration with  $\theta_{\frac{N}{2}+1} = \theta_{\frac{N}{2}}$  (in the absolute angles representation). In contrast, for odd  $N$  the condition  $\chi = 0$  implies  $\alpha_{\frac{N+1}{2}} = -\alpha_{\frac{N-1}{2}} \neq 0$  (in the relative angles representation), corresponding to an energetically disfavored configuration with  $\theta_{\frac{N+3}{2}} = \theta_{\frac{N-1}{2}}$  (in the absolute angles representation).

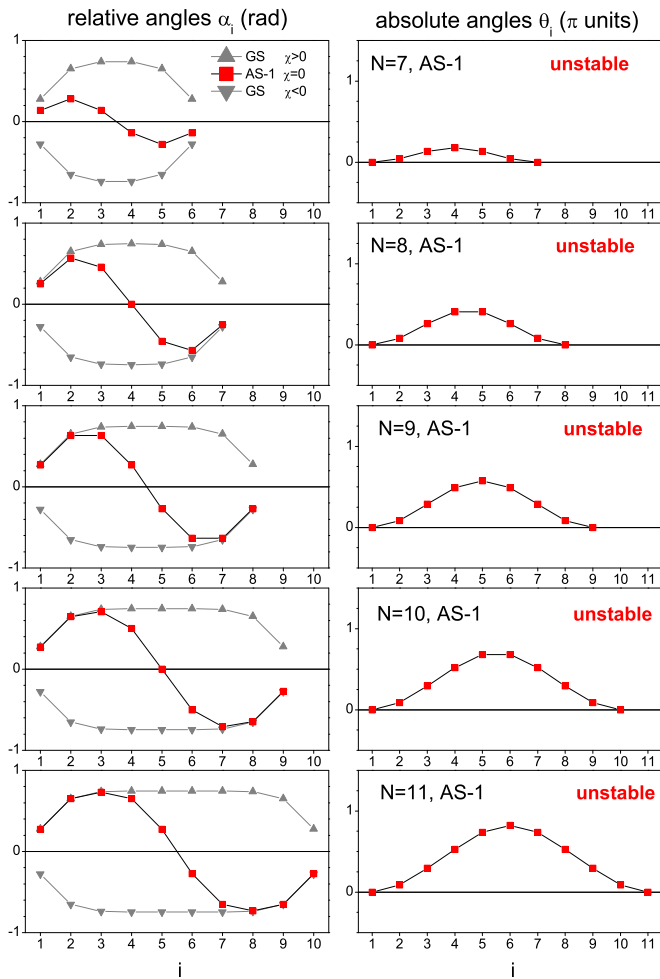


FIG. 5. (Color online) Unstable “antisymmetric” configurations, AS-1, of a chain with  $\gamma = -0.34$  and number of spins,  $N$ , ranging between 7 and 11. Left column: relative angles  $\alpha_i$  ( $i = 1, \dots, N-1$ ) of the AS-1 configuration (red squares) with  $\chi(N) = 0$  and of the two degenerate ground state configurations (gray triangles), with equal and opposite values of  $\chi(N) \neq 0$ . Right column: absolute angles  $\theta_i$  ( $i = 1, \dots, N$ ) of the AS-1 configuration. The lines are guides to the eye.

Note that this simple “rule of thumb” based on the parity of  $N$  is a sufficient condition for the metastability of the AS-1 state provided that the chain is long enough, in order that surface effects combined with the presence of the chiral domain wall are not so strong to drive the system very far from the ground-state configurations. In fact looking at Fig. 5, where the unstable AS-1 states for  $7 \leq N \leq 11$  are shown (red squares), one can notice that not only the spins in the middle of the chain (i.e., the spins belonging to the chiral domain wall) but also the spins near the end points of the chain have values of  $\alpha$  strongly perturbed with respect to the two ground states degenerate in energy and with opposite chirality (gray triangles). In contrast, for  $N \geq 12$  (see Fig. 6), in the AS-1 configuration all the spins of the chain, except those belonging to the chiral domain wall, have values of  $\alpha$  nearly indistinguishable from the two ground states.

In other words, for sufficiently high values of  $N$ , the AS-1 configuration represents a solution with  $\chi = 0$  that connects

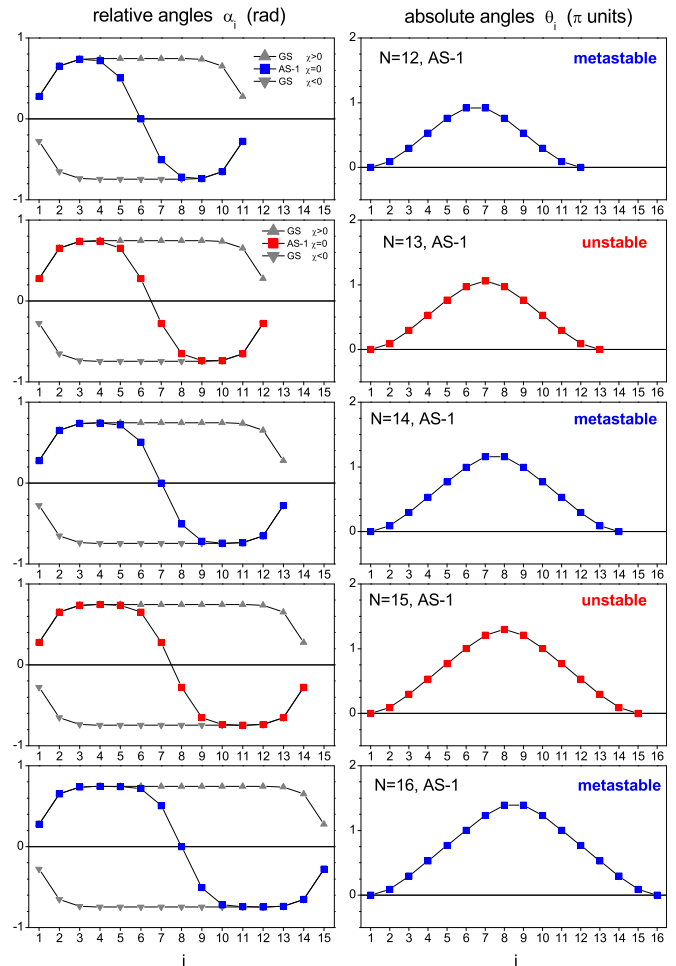


FIG. 6. (Color online) The same as in Fig. 5, but now the number of spins,  $N$ , ranges between 12 and 16. For these values of  $N$ , the “antisymmetric” configuration AS-1 turns out to be metastable for even  $N$ , and unstable for odd  $N$ .

two stable solutions, degenerate in energy, with equal and opposite values of  $\chi \neq 0$ . Then, if the energy cost of the chiral domain wall is not too high, the AS-1 configuration can be metastable. This concept will be further illustrated in Sec. IV in the framework of a nonlinear map representation of the problem. Finally we have calculated, in units of  $J_1$ , the energy cost of a chiral domain wall,  $\Delta E_w = E(AS-1) - E(GS)$ , as a function of  $N$ . For even  $N = 14$  and  $16$  we found  $\Delta E_w = 0.15424$ , while for odd  $N = 13$  and  $15$  the value was slightly higher,  $\Delta E_w = 0.15427$ . These results appear to be in good agreement with the numerical estimation performed years ago by Thomas and Wolf [35] in the case of the infinite chain (see Fig. 5 in their paper).

“Ugly” configurations. As regards “ugly” configurations of the type  $U_{\pm 1}$ , they are characterized by a chiral domain wall shifted away from the middle of the chain. This type of configuration can be metastable under the conditions to be specified later on. First we observe that in our model (6) there is no reason why an “ugly” configuration with a chiral domain wall shifted to the right ( $U_{+1}$ ) should have a different energy from an “ugly” configuration with a chiral domain wall shifted by the same amount to the left ( $U_{-1}$ ). The two states differ only

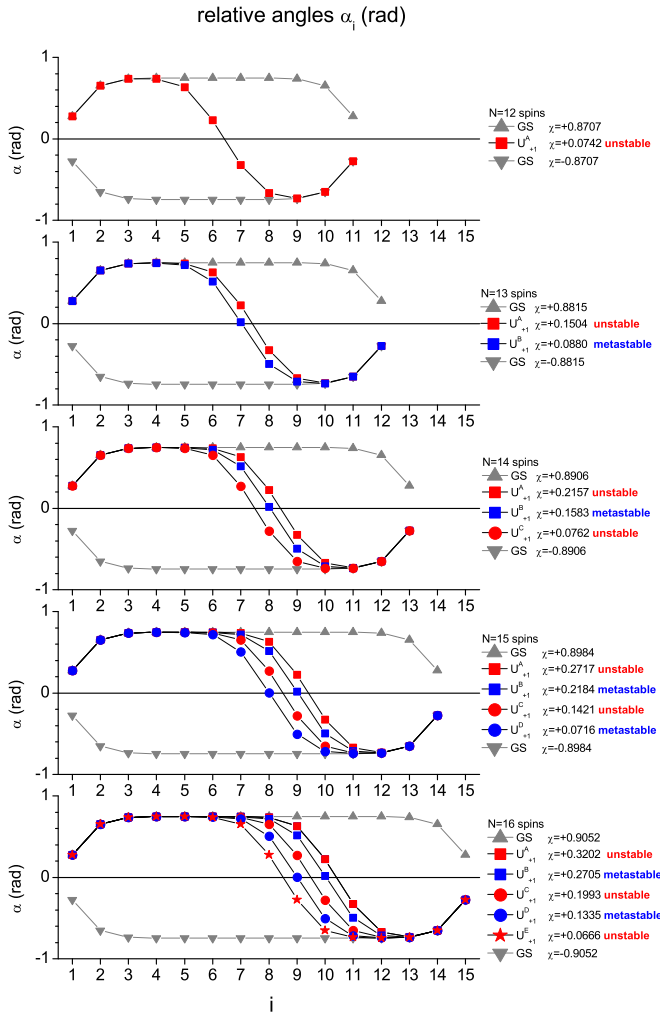


FIG. 7. (Color online) “Ugly” configurations  $U_+$ , with positive chiral order parameter  $\chi > 0$ , of a chain with  $\gamma = -0.34$  and number of spins,  $N$ , ranging between 12 and 16. Whenever the number of spins is increased by 1, an additional “ugly” state  $U_+$  is found, which is unstable for even  $N$  and metastable for odd  $N$ .

for the sign of the chiral order parameter ( $\chi > 0$  for  $U_{+1}$  and  $\chi < 0$  for  $U_{-1}$ ), while the absolute value is the same. This is the reason why “ugly” configurations always come in pairs with the same energy; see Figs. 1–3. It is important to note that this degeneracy is distinct from the one mentioned above, i.e., the one obtained making the transformation  $\alpha_i \rightarrow -\alpha_i$  with  $i = 1, \dots, N-1$ .

From Table I it appears that the higher the number of spins in the chain, the higher is the number of pairs of “ugly” metastable states one can observe. In Fig. 7 the various metastable states of a chain with  $\gamma = -0.34$  and variable number of spins,  $N$ , are shown in the relative angles representation,  $\alpha_i$  ( $i = 1, \dots, N-1$ ). For the sake of clarity, only “ugly” configurations  $U_+$ , with positive chiral order parameter  $\chi > 0$ , were drawn. One can notice that increasing values of the chiral order parameter correspond to increasing shifts of the chiral domain wall with respect to the middle of the chain. Regarding the stability of the “ugly” configurations, the latter is found to depend both on the number of spins in the chain and on the shift of the

chiral domain wall. More precisely, from Fig. 7 one can note that whenever the number of spins in the chain is increased by 1, a new “ugly” state is found, which is unstable for even  $N$  and metastable for odd  $N$ . As previously observed for the  $AS-1$  state, a sufficient condition for the metastability to be realized by an “ugly” state is that the chain is long enough, in order that surface effects combined with the presence of the chiral domain wall are not so strong to drive the system very far from the ground-state configurations. In fact from Fig. 7 it appears that metastable “ugly” configurations occur in correspondence of a *quasi*-vanishing relative angle,  $\alpha_{j_0} \approx 0$ , where  $j_0$  is an internal site which is shifted with respect to the middle of the chain. In terms of absolute angles, this means that one has two *quasi*-parallel nearest-neighbor spins,  $\theta_{j_0} \approx \theta_{j_0+1}$ . This represents an energetically favorable condition for the investigated case,  $\gamma = -0.34$ , where the antiferromagnetic nnn coupling does not dominate in the system.

#### IV. DISCRETE NONLINEAR MAP REPRESENTATION FOR THE STABLE CONFIGURATIONS OF THE CHAIN

In this section we give an alternative representation of the stable and metastable configurations in the form of trajectories in an appropriate phase space, using a discrete nonlinear map approach [24,30–32]. Following seminal works [33,34] on the Frenkel-Kontorova elastic model and the axial next-nearest-neighbor Ising (ANNNI) model, Belobrov *et al.* [24] performed the analysis of classical models of spin chains in the limit  $N \rightarrow \infty$ . They showed that the fixed points of the map are associated with commensurate configurations, while smooth and continuous curves (known as Kolmogorov-Arnold-Moser, KAM) in the space phase are associated with incommensurate configurations [24]. Under certain circumstances, it was shown [24] that a KAM curve can disintegrate into a chaotic set of points of the mapping, representing a disordered state of the chain. The presence of finite-size effects was first taken into account in a classical spin model by Trallori *et al.* [30,31], who showed that the equilibrium configurations of a finite open chain can be represented by trajectories of a nonlinear mapping satisfying opportune boundary conditions. The method was implemented to determine, within mean-field approximation, the stable and metastable states of a magnetic film in the presence of surfaces [30,31]. In particular, it was shown [32] that the effect of surfaces in the magnetic film model is equivalent to the introduction of a discommensuration in a Frenkel-Kontorova chain.

In the present work, we exploit the general topological properties of nonlinear maps to provide an overview of the equilibrium states of the system, both for  $N \rightarrow \infty$  and in the case of finite size [36]. Starting from Eq. (6), the equilibrium configurations for the open chain with  $N$  spins are given as usual by Eq. (9); clearly, in the thermodynamic limit the Kronecker’s  $\delta$  functions should be discarded. Introducing the auxiliary variables  $s_{i+1} = \sin(\alpha_i + \alpha_{i+1})$ , the equilibrium conditions of the chain can be rewritten in the form of a discrete nonlinear map in the  $(\alpha, s)$  phase space [24,30–32]

$$\begin{aligned} s_{i+1} &= -s_i - \frac{1}{\gamma} \sin \alpha_i, \\ \alpha_{i+1} &= -\alpha_i + \nu\pi + (-1)^i \psi, \end{aligned} \quad (14)$$



where  $\psi = \arcsin(s_{i+1})$  denotes the principal value of the function arcsin and  $\nu = 0, 1$  the branch index. To select the branch index, Belobrov *et al.* [24] proposed a criterion of local minimization for the free energy, while Trallori *et al.* [31,32], guessing the branch index to be a constant of the mapping, suggested that even in the case of a system with one or two surfaces the value of  $\nu$  to adopt is the one which reproduces the correct ground state for the associated infinite system. In the following, we will adopt the latter criterion.

The fixed points of the map are readily found to be

$$\begin{aligned} P_0 &= (\alpha_0, s_0) = (0, 0), \\ P_{\pm} &= \pm(\bar{\alpha}, \bar{s}) = \pm(\bar{\alpha}, \sin 2\bar{\alpha}), \end{aligned} \quad (15)$$

where  $\cos \bar{\alpha} = -\frac{1}{4\gamma}$ . It turns out that, for  $J_2/J_1 = \gamma < -1/4$ , the fixed point  $P_0$ , corresponding to the uniform ferromagnetic configuration, is energetically unstable and topologically stable (“elliptic” fixed point), while the fixed points  $P_{\pm}$ , corresponding to helical configurations with constant pitch and opposite chirality, are energetically stable and topologically unstable (“hyperbolic” fixed points). This is proved performing a linear stability analysis around the fixed points, i.e., finding the eigenvalues  $\lambda_{1,2}$  of the Jacobian matrix

$$\begin{aligned} \hat{J} &= \begin{pmatrix} \frac{\partial s_{i+1}}{\partial s_i} & \frac{\partial s_{i+1}}{\partial \alpha_i} \\ \frac{\partial \alpha_{i+1}}{\partial s_i} & \frac{\partial \alpha_{i+1}}{\partial \alpha_i} \end{pmatrix} \\ &= \begin{pmatrix} -1 & -\frac{1}{\gamma} \cos \alpha_i \\ \frac{-(-1)^\nu}{\sqrt{1-(s_i + \frac{1}{\gamma} \sin \alpha_i)^2}} & \frac{(-1)^\nu (-\frac{1}{\gamma} \cos \alpha_i)}{\sqrt{1-(s_i + \frac{1}{\gamma} \sin \alpha_i)^2}} - 1 \end{pmatrix} \end{aligned} \quad (16)$$

calculated in  $P_0$  and  $P_{\pm}$ , respectively.

In the eigenvalue equation

$$\lambda^2 - \text{Tr} \hat{J} \lambda + \det \hat{J} = 0 \quad (17)$$

one always has  $\det \hat{J} = 1$ ; i.e., the map is area-preserving in the  $(\alpha, s)$  phase space. In contrast,  $\text{Tr} \hat{J}$  depends on the fixed point. More precisely, one has the following:

(1)  $\text{Tr} \hat{J}|_{P_0} = -2 - \frac{1}{\gamma}$ , for the fixed point  $P_0$ . In this case, solving Eq. (17) one finds that for  $\gamma < -\frac{1}{4}$  the discriminant  $\frac{\Delta}{4} = (-\frac{1}{2} \text{Tr} \hat{J})^2 - 1 = \frac{1}{4\gamma^2} + \frac{1}{\gamma}$  is negative, meaning that the uniform ferromagnetic configuration is energetically unstable. The two eigenvalues  $\lambda_1$  and  $\lambda_2$  are complex conjugate and have modulus 1. The fixed point  $P_0$  is called elliptic because the map trajectories are closed orbits around it.

(2)  $\text{Tr} \hat{J}|_{P_{\pm}} = -2 + (-1)^\nu \frac{1}{4\gamma^2} \frac{1}{\sqrt{1-(\frac{1}{2\gamma} \sin \bar{\alpha})^2}}$ , for the fixed points  $P_{\pm}$ . In this case, solving Eq. (17) one finds that for  $\gamma < -\frac{1}{4}$  the discriminant is positive, provided that one takes the branch  $\nu = 0$  for  $0 < \bar{\alpha} < \frac{\pi}{4}$ , and the other branch  $\nu = 1$  for  $\frac{\pi}{4} < \bar{\alpha} < \frac{\pi}{2}$ . The condition  $\Delta > 0$  means that the two uniform helical configurations with pitch  $\pm \bar{\alpha}$ , degenerate in energy and with opposite chirality, are energetically stable. Equation (17) has two real eigenvalues, such that  $\lambda_1 > \lambda_2$  and  $\lambda_1 \lambda_2 = 1$ . Denoting by  $m_1$  ( $m_2$ ) the slope of the trajectory outflowing from (inflowing in) the hyperbolic fixed points  $P_{\pm}$ , one has ( $m_1 > m_2$ )

$$m_{1,2} = \left. \frac{\frac{\partial s_{i+1}}{\partial \alpha_i}}{\lambda_{1,2} - \frac{\partial s_{i+1}}{\partial s_i}} \right|_{P_{\pm}} = \frac{1}{\lambda_{1,2} + 1}. \quad (18)$$

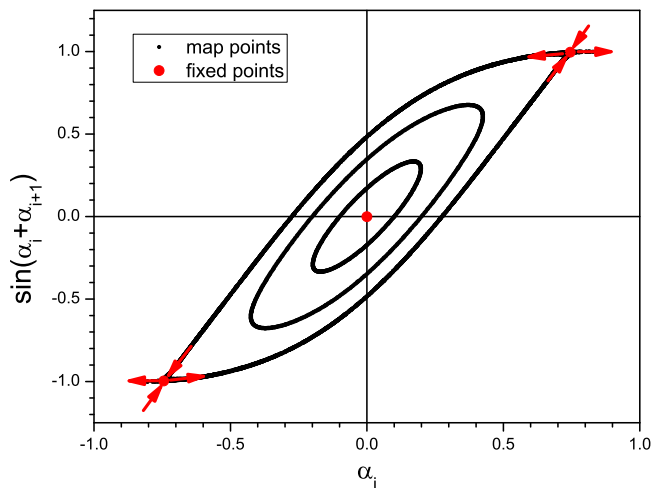


FIG. 8. (Color online) Phase portrait, obtained from the discrete nonlinear map Eqs. (14), for the classical planar spin chain in the case  $\gamma = -0.34$ . The red points  $P_0 = (0, 0)$  and  $P_{\pm} = \pm(\bar{\alpha}, \bar{s})$ , with  $\cos \bar{\alpha} = -1/(4\gamma)$  and  $\bar{s} = \sin 2\bar{\alpha}$ , denote the elliptic and the hyperbolic fixed points of the map, respectively. In the limit  $N \rightarrow \infty$ ,  $P_0$  and  $P_{\pm}$  correspond to the unstable collinear ferromagnetic state and to the stable helical states with constant pitch  $\pm \bar{\alpha}$ , respectively. Red arrows denote the direction of the map trajectories, with slopes given by Eq. (18), in the neighborhood of  $P_{\pm}$ .

The two elliptic trajectories encircling the fixed point  $P_0 = (0, 0)$  in Fig. 8 were obtained applying the direct map Eq. (14) to the points  $(0.1, 0)$  and  $(0.2, 0)$ . Also the heteroclinic orbit (i.e., the path in phase space which joins the two energetically stable fixed points  $P_{\pm}$ ) was obtained applying the direct map equation (14) to a collection of points chosen very near to  $P_{\pm}$  and lying on the line with smaller slope  $m_1$ . It should be noted that the branch  $\nu = 0$  was chosen in Eq. (14), according to the criterion by Trallori *et al.* [31,32]. In fact, for  $\gamma = -0.34$  one has that the choice  $\nu = 0$  reproduces the correct ground state of the infinite system.

Looking at Eqs. (9), it is apparent that for a finite chain with  $N$  spins the boundary conditions can be introduced in the nonlinear map via the two equations

$$\begin{aligned} s_1 &= \sin(\alpha_0 + \alpha_1) = 0, \\ s_N &= \sin(\alpha_{N-1} + \alpha_N) = 0, \end{aligned} \quad (19)$$

which involve two fictitious relative angles,  $\alpha_0$  and  $\alpha_N$ . In the map approach, an equilibrium configuration of the finite chain with  $N$  spins (i.e.,  $N - 1$  relative angles) and free ends is represented by a trajectory in the  $(\alpha, s)$  phase space, consisting of  $N$  discrete points, related one to the other by the iterative map Eqs. (14). It is important to note that, in order to satisfy the boundary conditions (19), the first and the last point of the trajectory must lie on the horizontal line,  $s = 0$ .

In Fig. 9 we show how the stable and metastable configurations of a finite open chain, obtained by the method described in Sec. II, appear in the  $(\alpha, s)$  phase space. (We remind the reader that for each of the configurations reported in Fig. 9, one can obtain another configuration, with the same energy and opposite chiral order parameter  $\chi$ , simply by replacing  $\alpha_i \rightarrow -\alpha_i$ .) We refer to an open chain of  $N = 14$  spins

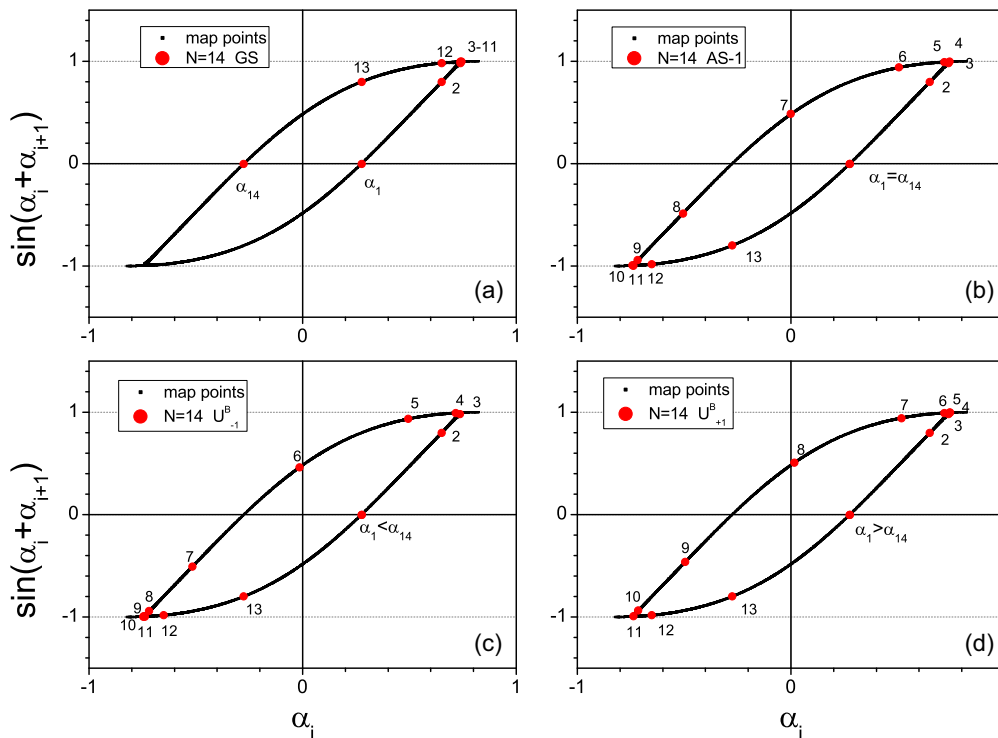


FIG. 9. (Color online) Nonlinear map representation of stable “symmetric”  $S$ -1 (ground state, GS), metastable “antisymmetric”  $AS$ -1, and metastable “ugly”  $U_{\pm 1}^B$  configurations of a finite chain with  $\gamma = J_2/J_1 = -0.34$  and  $N = 14$  spins. The physical relative angles are  $\alpha_i$  with  $i = 1, \dots, 13$ , while  $\alpha_{14}$  is a fictitious angle introduced to take into account open boundary conditions, Eq. (19), in the map formalism, Eq. (14).

with  $\gamma = -0.34$ , where the hyperbolic fixed points of the nonlinear map are  $P_{\pm} = \pm(\bar{\alpha}, \sin 2\bar{\alpha}) = \pm(0.7447, 0.9967)$ , and the slopes of the outflowing and inflowing trajectories are  $m_1 = 0.0846$  and  $m_2 = 2.0780$ , respectively.

(1) The ground state with positive chirality is depicted in Fig. 9(a). It is a trajectory of 14 points, many of them (3–11) lying very close to the hyperbolic fixed point  $P_+$ , which represents the helical ground state of the infinite chain with constant pitch  $+\bar{\alpha}$  and chiral order parameter  $\chi = +1$ . For a finite chain, the helix pitch depends on the position,  $i$ . All the physical relative angles  $\alpha_i$  ( $i = 1, \dots, 13$ ) are positive, leading to a configuration with  $\chi = 0.8906 > 0$ . The configuration is “symmetric” with respect to the middle of the chain since  $\alpha_{N-i} = \alpha_i$  for  $i = 1, \dots, 13$ . Clearly,  $\alpha_1$  and  $\alpha_{13}$  present the largest deviation from  $P_+$ . The angle  $\alpha_{14}$  (i.e., the last point of the map trajectory) is nonphysical and, for the GS with  $\chi > 0$ , it has the property that  $\alpha_{14} = -\alpha_1$ .

(2) The “antisymmetric” solution with one reversal of chirality is depicted in Fig. 9(b). It is a trajectory of 14 points (with the nonphysical angle  $\alpha_{14} = \alpha_1$ ) representing a configuration where the helix pitch  $\alpha_i$  depends on the position,  $i$ . The configuration is “antisymmetric” ( $\alpha_{N-i} = -\alpha_i$ ) with respect to the middle of the chain; for  $i = N/2$  the pitch vanishes exactly ( $\alpha_7 = 0$ ), separating the system into two regions with opposite chirality. The chiral order parameter of the configuration is then  $\chi = 0$ .

(3) The couple of metastable “ugly” solutions,  $U_{\pm 1}^B$ , are depicted in Figs. 9(c) and 9(d). Each of them is a trajectory of 14 points representing a configuration where the helix pitch varies from site to site. The chain is divided in two regions with opposite chirality. An “ugly” configuration is not “symmetric”

nor “antisymmetric” with respect to the middle of the chain. The pitch nearly vanishes at a site shifted to the left or to the right with respect to the middle of the chain ( $\alpha_6 \approx 0$  for the state  $U_{-1}^B$  and  $\alpha_8 \approx 0$  for the state  $U_{+1}^B$ ). Note that for “ugly” states the nonphysical angle  $\alpha_N$  is almost equal to  $\alpha_1$ , but does not coincide exactly with it. More precisely, one has  $\alpha_1 < \alpha_N$  for the  $U_{-1}^B$  state and  $\alpha_1 > \alpha_N$  for the  $U_{+1}^B$  state. From the map representation one can regard the equal and opposite values of the chiral order parameter, for the two “ugly” configurations  $U_{\pm 1}^B$  in the pair, as a direct consequence of the topological (and energetic) equivalence between the two hyperbolic fixed points,  $P_{\pm}$ . The “ugly” state  $U_{+1}^B$  ( $U_{-1}^B$ ) has  $\chi = 0.1583 > 0$  ( $\chi = -0.1583 < 0$ ) because more points of its trajectory are located near  $P_+$  ( $P_-$ ) than near  $P_-$  ( $P_+$ ). On the same grounds, one expects that the inclusion in the model of a chiral symmetry-breaking interaction, as the one in Eq. (8), would immediately remove the energetic degeneracy between the “ugly states”, because one of the two hyperbolic fixed points would be favored with respect to the other.

From the general topological properties of the nonlinear map depicted in Fig. 8 one has that, for the infinite chain, an isolated domain wall dividing the system into two regions with opposite chirality is represented by a heteroclinic orbit, i.e., a path in phase space which joins the fixed points  $P_{\pm}$ , corresponding to uniform (constant-pitch) helical configurations of the infinite chain. From Fig. 9 we observe that, for a finite chain with one chiral domain wall, the metastable configurations are associated with trajectories in phase space which (apart from the terminal points, and the points near the center which are involved in the chiral domain wall) have many representative points near  $P_{\pm}$ . Therefore, with increasing  $N$ ,

we expect configurations with an increasing number of chiral domain walls to appear and become metastable. Moreover, depending on the number of inversions of chirality being even or odd, these metastable states are expected to be “symmetric” or “antisymmetric”/“ugly”, respectively. Clearly, any distinction between even and odd features is expected to vanish for very long chains,  $N \gg \frac{2\pi}{\alpha}$  (i.e., in the limit where a continuum model for modulated states is expected to hold). We conclude this section by noticing that, in the quite different (nonmagnetic) context of stretched elastomer strips, metastable states with a single reversal or multiple reversals of chirality were indeed observed [16] and named “hemihelices”. In that case, the structural transition from a homohelical to a “hemihelical” shape of the strip, as well as the number of reversals of chirality (also named “perversions” [17]), was found to depend on the height-to-width ratio of the strip’s cross section. In the case of our model, it would be interesting to investigate whether a similar transition can occur, e.g., depending on the ratio,  $\gamma$ , between the competing nnn and nn exchange interactions and on the number,  $N$ , of spins in the chain.

## V. CONCLUSIONS

In conclusion, taking into account both the discrete nature and the finite size of a one-dimensional planar spin chain with competing nn and nnn exchange couplings, we were able to calculate in a very accurate way all the equilibrium states (stable, metastable, and unstable) of the system, using a theoretical method [28,29] recently developed. The calculations were performed for a particular value of  $\gamma$ , the ratio between nnn and nn couplings, which in the infinite chain leads to a constant-pitch and homochiral helical ground state. For chains with finite length (comparable with the period of helix modulation), the ground state was found to be a helix whose chirality is constant in sign along the chain, but whose pitch varies owing to finite-size effects. For finite but not too small values of the number of spins in the chain,  $N$ , we found metastable states characterized by one

reversal of chirality, either localized just in the middle of the chain [“antisymmetric” state, with chiral order parameter  $\chi(N) = 0$ ], or shifted away from the middle of the chain, to the right or to the left [pairs of “ugly” states, with equal and opposite values of  $\chi(N) \neq 0$ ]. Concerning the stability of these states with one reversal of chirality, two main results were found. First, the “antisymmetric” state is metastable for even  $N$  and unstable for odd  $N$ . Second, an additional pair of “ugly” states is found whenever the number of spins in the chain is increased by 1. The states in each additional pair are unstable for even  $N$  and metastable for odd  $N$ . Analysis of stable and metastable configurations in the framework of a discrete nonlinear mapping approach [24,30–32] provided further support to the theory, and suggested that also states with multiple reversals of chirality should become metastable with increasing the number of spins above the maximum value ( $N = 16$ ) considered in the present work.

## APPENDIX

In this appendix we provide a table with the calculated values of all nonzero solutions of equation  $F(\alpha_1) = 0$ , where the function  $F(\alpha_1)$  is defined in Eq. (13), for an open chain with  $N = 16$  spins and  $\gamma = -0.34$ . We found 14 positive roots which are reported in the second column, denoted by the label  $\alpha_1^{(0)}$ . The third column specifies the type of magnetic structure associated with the root (whether “symmetric”, “antisymmetric”, or “ugly”), and the fourth column its stability. Finally, the fifth column specifies the energy of the configuration.

In the numerical calculations, the computer time required to find the first orientation angle was found to increase with increasing  $N$ . For  $N = 16$  (the longest investigated chain length), using an ordinary pc the computer time needed to find a root  $\alpha_1^{(0)}$  with 30 digits was nearly 30 minutes. We note that such a high number of digits in the first orientation angle is necessary to get the other angles with enough precision [37], so as to recognize the peculiar symmetry properties of the various stationary configurations reported in Sec. III, and to perform the analysis of stability in a reliable way.

TABLE II. The 14 positive roots,  $\alpha_1^{(0)}$  (2nd column), of the function  $F(\alpha_1)$  defined in Eq. (13), calculated for an open chain with  $N = 16$  spins and  $\gamma = J_2/J_1 = -0.34$ ; the related type of configuration (3rd column); the stability (4th column); the reduced energy  $\epsilon$  (5th column), calculated using Eq. (11).

Root	$\alpha_1^{(0)}$ (rad)	Type	Stability	Energy $\epsilon$ (units of $J_1$ )
1	0.139439046248061848676383222937	AS-2	unstable	-10.2429411764705882352941156471
2	0.264491481382757534472060225654	S-2	unstable	-10.3428549058518829959680256709
3	0.275194885065826086527846629266	$U_{-1}^A$	unstable	-10.6461824282207617918810701027
4	0.275321854471931262846053070159	$U_{-1}^B$	metastable	-10.6462000922017083463635002161
5	0.27536809949097186444604357678	$U_{-1}^C$	unstable	-10.6461596868684236550328388525
6	0.275376350686316961814821188590	$U_{-1}^D$	metastable	-10.6461943155339302495063290620
7	0.275378058752456471531424476243	$U_{-1}^E$	unstable	-10.6461585756941485144576441228
8	0.275378403443466744841988143120	AS-1	metastable	-10.6461940980319102697850279786
9	0.275378472763985432104826993291	$U_{+1}^E$	unstable	-10.6461585756941485144576441227
10	0.275378486841454490886111372119	$U_{+1}^D$	metastable	-10.6461943155339302495063290619
11	0.275378489640898454584912451796	$U_{+1}^C$	unstable	-10.6461596868684236550328388526
12	0.275378490238027539108091622662	$U_{+1}^B$	metastable	-10.6462000922017083463635002162
13	0.275378490329487734339367590766	$U_{+1}^A$	unstable	-10.6461824282207617918810701026
14	0.275378490369573279440991374919	S-1	stable (GS)	-10.8004322041729081015840664838

From Table II one observes that, for  $N = 16$ , the first five excited metastable states are quasidegenerate. However, by the method described in Sec. II it is impossible to determine the energy barriers that separate local minima from the global minimum and/or from each other. In fact, the method does not allow one to explore the details of the energy landscape in the  $N$ -dimensional space because one judges about that landscape on the basis of the behavior of a function of only one argument,  $\Phi(\alpha_1)$  in Eq. (11), which has “spurious” minima in addition to “true” ones. Using the data reported in Table II, one can only estimate the energy cost of a chiral domain wall,  $\Delta E_w$ . As a consequence of the finite size of the chain,  $\Delta E_w$  is found to weakly depend on the location of

the wall with respect to the middle of the chain: the closer the wall is to the free ends of the chain, the lower is the value of  $\Delta E_w$ . In fact, for the  $AS - 1$  “antisymmetric” state, with a chiral domain wall located just at the middle of the chain, we find  $E(AS - 1) - E(GS) = \Delta E_w = 0.15423811$  (in units of  $J_1$ ); for the  $U_{\pm 1}^D$  “ugly” states, with the chiral domain wall shifted by nearly one lattice site from the middle of the chain, the energy difference is a bit lower,  $E(U_{\pm 1}^D) - E(GS) = \Delta E_w = 0.15423789$ ; finally, for the  $U_{\pm 1}^B$  “ugly” states, with the chiral domain wall shifted by nearly two lattice sites from the middle of the chain, the energy difference is further lowered,  $E(U_{\pm 1}^B) - E(GS) = \Delta E_w = 0.15423211$ .

- 
- [1] J. Jensen and A. R. Mackintosh, *Rare Earth Magnetism: Structures and Excitations* (Clarendon Press, Oxford, 1991).
- [2] P. A. Herpin and P. Meriel, *J. Phys. Radium* **22**, 337 (1961).
- [3] L. Udvardi, S. Khmelevskiy, L. Szunyogh, P. Mohn, and P. Weinberger, *Phys. Rev. B* **73**, 104446 (2006).
- [4] A. Yoshimori, *J. Phys. Soc. Jpn.* **14**, 807 (1959).
- [5] J. Villain, *J. Phys. Chem. Solids* **11**, 303 (1959).
- [6] T. A. Kaplan, *Phys. Rev.* **116**, 888 (1959).
- [7] J. Villain, *J. Phys. II (France)* **38**, 385 (1977).
- [8] H. Kawamura, *J. Phys. Condens. Matter* **10**, 4707 (1998).
- [9] F. Cinti, A. Rettori, M. G. Pini, M. Mariani, E. Micotti, A. Lascialfari, N. Papinutto, A. Amato, A. Caneschi, D. Gatteschi, and M. Affronte, *Phys. Rev. Lett.* **100**, 057203 (2008).
- [10] Yu A. Izyumov, *Sov. Phys. Usp.* **27**, 845 (1984).
- [11] H. Hubert, *Theorie der Domänenwände in geordneten Medien*, Lecture Notes in Physics Vol. 26 (Springer-Verlag, Berlin, 1974), p. 327.
- [12] P. I. Melnichuk, A. N. Bogdanov, U. K. Roessler, and K.-H. Mueller, *J. Magn. Magn. Mater.* **248**, 142 (2002).
- [13] S. Aubry, *J. Phys. (France)* **44**, 147 (1983).
- [14] I. Markov and A. Trayanov, *J. Phys. Condens. Matter* **2**, 6965 (1990).
- [15] S. L. Shumway and J. P. Sethna, *Phys. Rev. Lett.* **67**, 995 (1991).
- [16] J. Liu, J. Huang, T. Su, K. Bertoldi, and D. R. Clarke, *PLoS One* **9**, e93183 (2014).
- [17] T. McMillen and A. Goriely, *J. Nonlinear Sci.* **12**, 241 (2002).
- [18] E. Weschke, H. Ott, E. Schierle, C. Schussler-Langeheine, D. V. Vyalikh, G. Kaindl, V. Leiner, M. Ay, T. Schmitte, H. Zabel, and P. J. Jensen, *Phys. Rev. Lett.* **93**, 157204 (2004).
- [19] K. Dumesnil, *Collection SFN* **13**, 04002 (2014).
- [20] F. Cinti, A. Cuccoli, and A. Rettori, *Phys. Rev. B* **83**, 174415 (2011).
- [21] L. D. Pan, S. Wang, C. S. Hsu, and C. C. Huang, *Phys. Rev. Lett.* **103**, 187802 (2009).
- [22] G. Chen, J. Zhu, A. Quesada, J. Li, A. T. N’Diaye, Y. Huo, T. P. Ma, Y. Chen, H. Y. Kwon, C. Won, Z. Q. Qiu, A. K. Schmid, and Y. Z. Wu, *Phys. Rev. Lett.* **110**, 177204 (2013).
- [23] M. Menzel, Y. Mokrousov, R. Wieser, J. E. Bickel, E. Vedmedenko, S. Blugel, S. Heinze, K. von Bergmann, A. Kubetzka and R. Wiesendanger, *Phys. Rev. Lett.* **108**, 197204 (2012).
- [24] P. I. Belobrov, V. V. Beloshapkin, G. M. Zaslavskii, and A. G. Tret’yakov, *Zh. Eksp. Teor. Fiz.* **87**, 310 (1984) [*Sov. Phys. JETP* **60**, 180 (1984)]; and references therein.
- [25] I. E. Dzialoshinskii, *Zh. Eksp. Teor. Fiz.* **35**, 1547 (1957) [*Sov. Phys. JETP* **5**, 1259 (1957)].
- [26] T. Moriya, *Phys. Rev.* **120**, 91 (1960).
- [27] M. Bode, M. Heide, K. von Bergmann, P. Ferriani, S. Heinze, G. Bihlmayer, A. Kubetzka, O. Pietzsch, S. Bluegel, and R. Wiesendanger, *Nature (London)* **447**, 190 (2007).
- [28] A. P. Popov, A. V. Anisimov, O. Eriksson, and N. V. Skorodumova, *Phys. Rev. B* **81**, 054440 (2010).
- [29] A. P. Popov, *J. Magn. Magn. Mater.* **324**, 2736 (2012).
- [30] L. Trallori, P. Politi, A. Rettori, M. G. Pini, and J. Villain, *Phys. Rev. Lett.* **72**, 1925 (1994).
- [31] L. Trallori, M. G. Pini, A. Rettori, M. Macciò, and P. Politi, *Int. J. Mod. Phys. B* **10**, 1935 (1996).
- [32] L. Trallori, *Phys. Rev. B* **57**, 5923 (1998).
- [33] S. Aubry, *Solitons and Condensed Matter Physics*, edited by A. R. Bishop and T. Schneider (Springer-Verlag, Berlin, 1979), pp. 264–290.
- [34] P. Bak, *Rep. Prog. Phys.* **45**, 587 (1982).
- [35] H. Thomas and P. Wolf, in *Proceedings of the International Conference on Magnetism, Nottingham, September 1964* (Physical Society and Institute of Physics, London, 1965), pp. 731–734.
- [36] Note that in principle one can use the nonlinear map method also to calculate the stable configurations. However, in the present work, this task was accomplished using the theoretical method described in Sec. II.
- [37] To be more specific, with 30 digits in the first orientation angle, we were able to get the last orientation angle with a very good accuracy,  $10^{-19}$ , whereas with 20 digits the accuracy was  $10^{-10}$ .